Reliability analysis of tape based chip-scale packages based metamodel

Hamid Hamdani, Abdelkhalak El Hami, Bouchaïb Radi

Version of Record: https://www.sciencedirect.com/science/article/pii/S0026271419301039
Manuscript_76e3752407d5671504fc6999a988ee38

Reliability analysis of Tape based Chip-Scale packages based Metamodel

Hamid HAMDANI[a,b,*], Abdelkhalak EL HAMI[a], Bouchaïb RADI[b]

[a] *LMN, Normandie Univ, INSA Rouen, 76000 Rouen, France*

[b] *LIMII, FST Settat, BP: 577, Route de Casa, Settat, Morocco*

Abstract

In the mechatronic devices, finite element methods (FEM) are widely used to determine the fatigue response of solder joints subjected to thermal loading. These life cycle analyses are often deterministic. However, experience shows that design variables present variability that affects prediction quality. This paper describes a method for predicting the solder joints reliability in Tape based Chip Scale Packaging (T-CSP) with consideration of uncertainties in material properties. The proposed approach, which is based on the metamodelling techniques, combines FEM, metamodels and Monte Carlo Simulation (MCS). Once validated, the constructed metamodel is used to perform the MCS. This probabilistic method has sufficient efficiency and accuracy to analyze the reliability of T-CSPs.

Keywords: Chip-Scale Packages, Finite-element analysis, Kriging metamodel, Monte-Carlo Simulation, Solder joint

1. Introduction

Using Chip Scale Packaging (CSP) technologies in electronic products is rising because of the increasing demand for smaller and more portable electronic devices. Specifically, in CSP, the footprint of the package does not exceed 120 % of the size of the silicon chip that has been inserted [36]. The main advantage of CSPs over traditional Ball Grid Array (BGA) electronic packaging technologies is that they save considerable space. CSP technologies can be classified into four categories: Flex or Tape where chips are deposited on a tape or flexible material. Rigid (chips rest on a laminated or ceramic substrate), Lead frame (chips are deposited on a frame) and Wafer Level. In this work, Tape based chip-scale package technology (T-CSP) was studied. Under operating conditions, electronic devices are subject to wide temperature variations. The thermomechanical stresses in solder joints because of the difference in material properties, Coefficient of Thermal Expansion (CTE) mismatch between the multiple materials involved in the construction of a typical package, may lead to damage and hence the failure of the solder joints.

Finite element methods (FEM) are used during the development phase of mechatronic products to improve the reliability of microelectronic packaging. They can provide a detailed description of solder stress/strain history and distribution under various loading conditions. Many researches about the characterization of thermomechanical reliability have been implemented on the basis of FEM simulation [29, 25, 31, 5, 24, 22]. In engineering applications, the analyst is interested in predicting the number of fatigue life cycles, i.e. the number of cycles that the packaging can resist before failure [12, 13]. Consequently, a combination of finite element methods with a thermal fatigue model is required. Several

*I am corresponding author
Email addresses: hamid.hamdani@insa-rouen.fr (Hamid HAMDANI), abdelkhalak.elhami@insa-rouen.fr (Abdelkhalak EL HAMI), bouchaib.radi@yahoo.fr (Bouchaïb RADI)

methodologies based on FEMs have been proposed to predict the solder joint life cycles. These approaches can be classified into four categories. They are based on stress or plastic deformation and creep, or energy or damage [19]. Darveaux's energy-based approach [5] is the most widely used one, because of the facility of its implementation. In this approach the number of cycles to initiate a crack, and the number of cycles for the crack to propagate across a solder joints diameter are expressed as a function of the strain energy density accumulated per cycle during thermal cycling. The accuracy of Darveaux's methodology has been evaluated and validated in several electronic assembly studies. This approach has become a technical reference for this type of complex physical analysis.

Generally, the used simulation tools, for predicting the reliability of T-CSPs, are based on deterministic approaches, which do not take into account the variability and randomness of input parameters and operational conditions. For example, in [36], particular attention was paid to studies of the impact of the variation in T-CSP configurations on the reliability of solder joints, this difference in configurations is due to both tape vendors and package assembly on the devices reliability. However, this type of study does not take into account the natural variability of the material parameters and the manufacturing process. Therefore, it is necessary to perform an uncertainty analysis, which estimates reliability from uncertain inputs [17]. In this paper, the material properties are considered as random variables and their influence on the reliability of the entire package is analyzed.

Probabilistic, non-probabilistic, and analytical methods are the three main categories of methods for uncertainty analysis [14]. Monte Carlo simulation (MCS) method classified in the probabilistic methods is the most used one. Typically, MCS relies on repeated random sampling of the input variables to obtain multiple outputs results. In the MCS method, thousands even millions of deterministic simulations are performed based on a large number of samples in order to obtain precise results.

The complex nonlinear finite element analysis of T-CSP take more time to determine the time-dependent solder joint fatigue response, consequently, using MCS to analysis the uncertainty in the reliability prediction of CSP, will be computationally expensive. In order to efficiently overcame the computational cost, metamodel based probabilistic method is proposed an applied to evaluate the reliability of CSP while taking into account the variability of material parameters. The proposed method combines metamodel[11, 7], MCS and FEM simulation. More precisely, three-dimensional finite element analysis has been applied to determine the time-dependent solder joint fatigue response of a T-CSP under loading conditions, then the appropriate metamodel is built based on the inputs parameters and theirs responses from deterministic FEM simulations. Subsequently, the constructed metamodel is used to perform the MCS.

2. Description of the studied Tape based chip scale package

The device analyzed is a 13x13mm CSP. This device is composed of 225-ball (15x15 full ball matrix), with 0.80mm pitch and a die size which was measured at 8.24x9.12mm. The used Tape technology allows the connection of a chip with bumps on a flexible circuit (Figures 2). This technique is used mainly in the LCD display industry to assemble drivers or for optical applications such as stepper motor sensors.

In [35] the adopted T-CSP shown in figure 1.**a** was analyzed by the finite element method, the author was study the impact of Eight differing ball via configurations on solder joint reliability, these configurations are due to the variations in both tape vendors and package assembly. All the studied packages consisted of a 1-metal layer tape substrate and incorporated a 0.380mm substrate solder pad diameter with a solder ball via hole opening diameter of 0.280mm at the tape metal layer pad. The stackup layer thickness information for the Printed Circuit Board (PCB) is provided in figure1.**b**. The present study aims to analyse the first configuration [35], by considering the uncertainties resulting from material properties and the thermal expansion mismatch of the different materials in the T-CSP configurations.

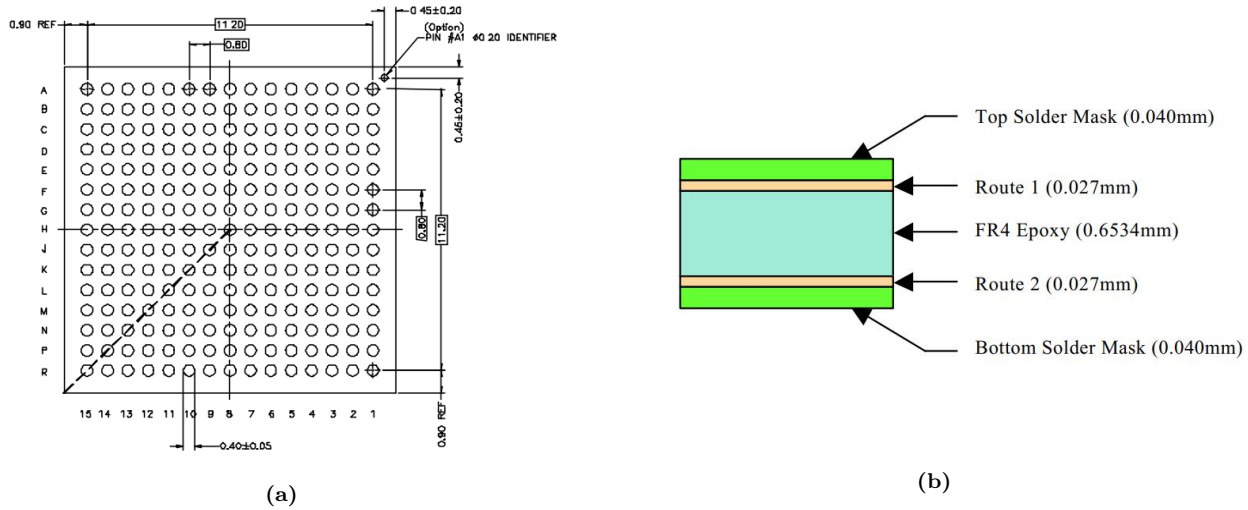

Figure 1: Package outline drawing (a) and Layer dimensions of pcb (b)

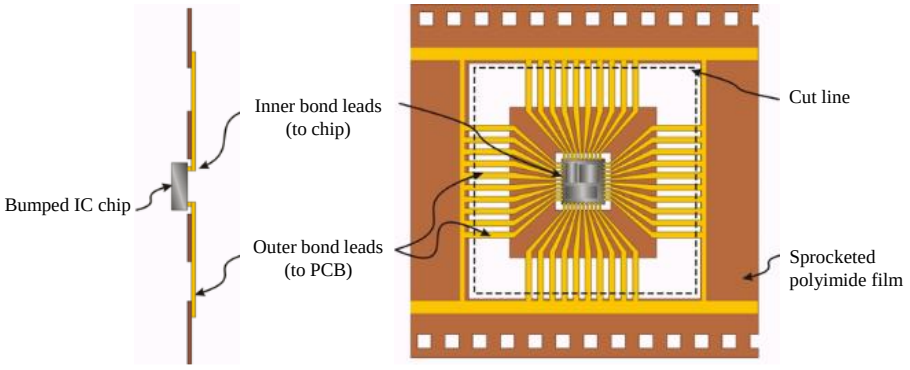

Figure 2: Principle of Tape automated bonding

2.1. Material Properties

In the thermomechanical analysis of the studied T-CSP, several material properties were incorporated which varies from plastic and elastic, linear and non-linear, dependent or independent of material properties on time and temperature. For solder joint materials, the development of plastic strains is dependent on the rate of loading. Many authors have studied the response of solder joints and proposed constitutive equations. Anand's constitutive model [1] which incorporates viscoplasticity, is one of the developed equations.

Anand model expresses the material viscoplastic behavior that unifies creep and plasticity. However, Anand's model does not take into account the rate independent plasticity phenomenon. In this way, Darveaux [4] has modified the constants in Anand's constitutive model to take into consideration both time independent and time-dependent phenomena. Table 5 shows the modified Anand constants that were activated for the solder ball material of the studied CSP.

Component (Material)	**Elastic Modulus (MPa)**	**Shear Modulus (MPa)**	**CTE (1/K)**	**Poisson's Ratio (No Units)**
Ball (63Sn37Pb)	$75842 - 152T$	–	24.5×10^{-6}	0.35
Chip (Silicon)	162716	–	$-5.88 \times 10^{-6} + 6.26 \times 10^{-8}T - 1.6 \times 10^{-10}T^2 + 1.5 \times 10^{-13}T^3$	0.28
Conductor (Copper)	128932	–	$13.8 \times 10^{-6} + 9.44 \times 10^{-9}T$	0.34
PCB Core (FR4)	$27924 - 37T$(XY) $12204 - 16T$(Z)	$12600 - 16.7T$(XY) $5500 - 7.3T$(YZ&XZ)	16.0×10^{-6}(XY) 84.0×10^{-6}(XY)	0.39(XZ&YZ) 0.11(XY)
PCB Mask (Dry Film)	4137	–	30.0×10^{-6}	0.40

T=Material Property Temperature in Kelvin

Table 1: Model Material Properties

T=Tape (Kapton-E)			
Temp (K)	**Elastic Moduli (MPa)**	**CTE (1/K)**	**Poisson's Ratio (No Units)**
233	6624	(XY) 1.20×10^{-5} (Z) 3.00×10^{-5}	0.32
298	5520		0.34
423	1252		0.33
448	313		0.32

Table 2: Tape Material Properties

Die Attach (84-3MVB)			
Temp (K)	**Elastic Moduli (MPa)**	**CTE (1/K)**	**Poisson's Ratio (No Units)**
233	12184	4.40×10^{-5}	0.35
298	6769	4.50×10^{-5}	0.35
353		7.90×10^{-5}	
363		8.90×10^{-5}	
368		9.90×10^{-5}	
373		1.33×10^{-4}	
383		1.34×10^{-4}	
473	207	3.00×10^{-5}	0.35

Table 3: Die Attach Material Properties.

Mold Compound (EME7730)			
Temp (K)	**Elastic Moduli (MPa)**	**CTE (1/K)**	**Poisson's Ratio (No Units)**
233	28224	9.00×10^{-6}	0.25
298	23520		0.25
403		1.00×10^{-5}	
418		1.70×10^{-5}	
423		2.20×10^{-5}	
428		2.70×10^{-4}	
443		3.40×10^{-4}	
473		3.50×10^{-5}	0.35
513	1764		0.35

Table 4: Mold Compound Material Properties.

Parameters		Value	Description
A	(S^{-1})	410^6	Pre-exponential factor
Q/R	(K)	9400	Q = activation energy,R = university energy
ξ	(dimensionless)	1.5	Multiplier of stress
m	(dimensionless)	0.303	Strain rate sensitivity of stress
$\hat{s}$	(dimensionless)	73.81	Coefficient for deformation resistance saturation value
n	(dimensionless)	0.07	Strain rate sensitivity of saturation value
h_0	(MPa)	1378.95	Hardening constant
a	(dimensionless)	1.3	Strain rate sensitivity of hardening of softening
s_0	(MPa)	12.41	Initial value of deformation resistance

Table 5: Darveaux Modified Anand Constants [4]

3. Proposed reliability method based Metamodel

In the reliability assessment, uncertainty analysis is performed with probabilistic methods such as Monte Carlo simulation. MCS consist in generating the input range from a distribution of input variables using one of the sampling methods, then the sampling results are used to calculate the responses (outputs) of the finite element model. However, to obtain more accurate results, MCS requires a large number of inputs samples. In the thermomechanical simulation, the non-linear transient finite element analysis such as reliability analysis of , encompass a complex physics, which makes the simulation computationally expensive. Consequently, the classic MCS becomes impractical. For this reason, the metamodel based probabilistic method is proposed to overcome the deficiency of computational cost. In this proposed method, the thermomechanical simulation is approximated by a metamodel.

The most common way to define a metamodel is to consider it as a model of the model. Metamodels can be found under other names such as emulator, approximator, surrogate model, simplified model or response surface. The metamodeling process consists in constructing an approximation function $\hat{y}(\mathbf{x})$ that adequately represents the relationship between the given input data points $\mathbf{S} = \left[\mathbf{x}^{(1)}, \mathbf{x}^{(2)}, \ldots, \mathbf{x}^{(n)}\right]^{T}$, and their corresponding output values computed using the complex model (FE model)$\mathbf{y}_s = \left[y\left(x^{(1)}\right), y\left(x^{(2)}\right), \ldots, y\left(x^{(n)}\right)\right]^{T}$. The set of input data points is generated by the design of experiments (DOE) strategy. The main objective is to be able to explore a complex model more easily and to be able to evaluate and simplify it much more quickly. several metamodeling approaches have been used in recent research, such as support vector regression, radial basis functions, polynomial regression, and Kriging metamodel. Polynomial regression (PR), which uses a polynomial to approximate the function, is the most easily used kind of metamodel. The quadratic response surface is the popular form of polynomial regression model. however, using lower order polynomials, it is not easy to approximate a non-linear function globally with a high accuracy. Recently, high-order polynomials [20] such as the Bernstein polynomials, Chebyshev polynomials[33] and Gegenbauer functions have been attempted

to be used for metamodelling [34]. support vector machines (SVMs) and support vector regression (SVR) are a powerful technique in machine learning. Radial basis functions (RBFs) represent metamodels as linear combinations of a particular type of basis function [18]. Kriging metamodel can be seen as the realisation of a gaussian process and is one of the most used and powerful metamodels. From the various kinds of metamodel, we need to choose the appropriate one for FE model approximation. In many works, the Kriging metamodel is proved as a powerful tool to approximate nonlinear computer code[16]. The Kriging metamodel is chosen in the proposed probabilistic approach.

3.1. Kriging metamodel

Kriging is a geostatistical technique to interpolate deterministic noise-free data. The theory of kriging has been formalised by the mathematician Matheron [23], Subsequently, Kriging has become a standard method for constructing metamodels for computer experiments [27]. It is then used to predict the value of an expensive fitness function (FE model). This method is also known as Gaussian process regression. Let $y(x)$ be defined as a function of x, with $x \in R_d$ and y is a vector of n observed values of $y(x)$ on $D = \{x_1, \ldots, x_n\}$, a design of experiment(DOE) with dimension $n * d$. Kriging assumes that the function $y(x)$ is a realisation of a Gaussian process denoted by $Y(x)$, which is given as :

$$Y(x) = h(x) + Z(x) \tag{1}$$

where $h(x)$ is the mean of the process, and $Z(x)$ is a Gaussian process with zero mean and covariance expressed by:

$$\mathrm{Cov}(Z(x^{(i)}), Z(x^{(j)})) = \sigma^2 R(x^{(i)}, x^{(j)}) \text{ for } i, j = 1, .., N \tag{2}$$

with σ^2 is the variance of Gaussian process and $R(x^{(i)}, x^{(j)})$ its correlation function between any two samples $x^{(j)}$ and $x^{(j)}$.

The choice of the correlation function is an important element of kriging. Many covariance functions are proposed in the literature [26], such as matter, Gaussian, exponential or spherical correlation functions. The Gaussian correlation function is the most commonly used; this last allows control of both the range of influence and the smoothness of the approximation model:

$$R(x^{(i)}, x^{(j)}) = \exp\left[\sum_{k=1}^{d} -\theta_k \left| x_k^{(i)} - x_k^{(j)} \right|^2\right] \tag{3}$$

where d is the dimension of design space, $\theta_k (k = 1, 2, ..., d)$ are unknown parameters of the correlation function, $x_k^{(i)}$ and $x_k^{(j)}$ respectively are the k^{th} component of the sampling point x_i and x_j.

for any new point x, The mean and variance of prediction [27] can be respectively calculated by:

$$\hat{y}(x) = h^T(x)\beta + r^T(x)R^{-1}(y - H\beta) \tag{4}$$

$$s^2(x) = \sigma^2 \left[r^T(x)Rr(x) + \frac{1 - I^T(x)R^{-1}r(x)}{1 - I^T(x)R^{-1}I} \right] \tag{5}$$

where $\hat{y}(x)$ and $s^2(x)$ are respectively the estimated mean value and variance of $\hat{y}(x)$, $h^T = [h_i], i = 1, \ldots, k$ a set of basis functions (e.g. polynomial functions), $\beta = (\beta_1, ..., \beta_k)$ the associated regression coefficients, R is the correlation matrix of D, and H the matrix corresponding to the values of $h^T(D)$, and $r(x) = [R(x, x_1), \ldots, R(x, x_k)]^T$ is the vector of correlation functions between the untried point x and the k samples $x^{(1)}, ..., x^{(k)}$.

The unknown model parameters can be determined using likelihood estimates (MLEs) method [30]

3.2. Proposed metamodel based probabilistic method

The proposed method aims to combine the metamodeling techniques with Monte Carlo simulation to perform uncertainty analysis with high efficiency. The proposed method use the design of experiment to generate the sampling inputs, and the deterministic finite element analysis is executed for each of sampling inputs, then the metamodel is used to represent the relationship between the sampling input and the calculated outputs. Finally, the MCS is realized based on the construct metamodel. The procedure of the proposed method can be summarized in four steps:

1. Generate the sampling inputs based on the one of design of experiment method ;
2. Obtain the response values through FEM simulation by using the sampled inputs ;
3. Chose, Construct ans validate the metamodel ;
4. Use the construct metamodel to perform Monte Carlo simulation.

For the implementation of the metamodel based probabilistic method, the interconnection between R programing [32] and ANSYS [2] is performed in order to combine the MCS, metamodel and finite element analysis. Figure 3 shows the flowchart of the method implementation.

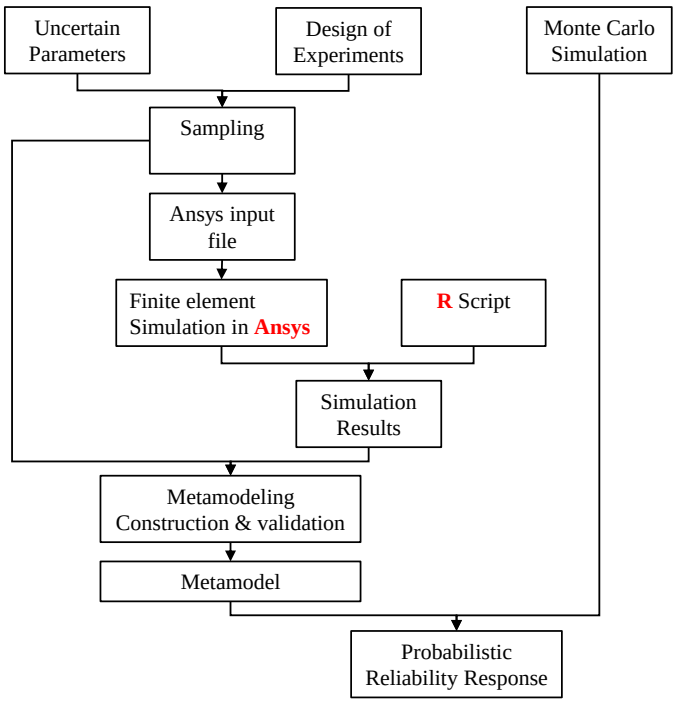

Figure 3: Flow chart of the proposed reliability method.

4. Deterministic FEM simulation of T-CSP

4.1. Solder Balls finite element model

The main objective of the deterministic study is to predict solder joint reliability of T-CSP using finite element simulation methods. For the purpose of avoiding tedious computation due to the complexity of physics which includes this kind of non-linear finite element analysis, only the diagonal slice of the studied package was developed [35]. The use of the diagonal slice, shown by the bold print dashed line in figure 1, ensures the simulation of the worst-case situation in which the solder ball is located at the

furthest distance from the center neutral point of the package. The figure 4 shows the perspective view of the meshed 3D diagonal slice model developed by ANSYS Finite Element Analysis software [2]. The structured (mapped) finite element mesh is adopted. The configuration detail is provided in table 6.

As shown in Figure 1.**a**, the studied slice model contains a full set of solder joints and all major components, crossing the entire thickness of the package assembly. For the boundary constraints, the plane of the slice model is neither a true symmetry plane nor a free surface i.e. the surface of the slice plane must remain planar and free to move in the y direction. For this reason, coupling the y-displacements of the nodes on the slice plane was chosen. Figure 4 shows the boundary constraint applied to the numerical model. For the present analysis, the width of the slice model was set at one-half the solder ball pitch and the length PCB (x-dimension) was set at 1.5 that of the modeled package slice x-dimension. The ball pitch of the diagonal slice model is the hypotenuse (1.1314mm) of the true ball pitch (0.80mm).

Mold Cap	Die	Die Attach	Metal Layer	Adhesive Layer	Tape Substrate	Via Type
0.7mm EME7730	0.3048mm Silicon	0.0445mm 84-3MVB	0.025mm Copper	N/A	0.050mm Kapton-E	Generic Etched
Via Plug	Via Hole Top Dia.	Via Hole Bottom Dia.	Substrate Joint Dia.	PCB Joint Dia	Solder Ball Stdoff. Ht.	Solder Ball Ctr. Dia.
N/A	0.2800mm	0.4206mm	0.2800mm	0.2800mm	0.2860mm	0.4640mm

Table 6: Tape Based Chip-Scale Package configuration Details [36].

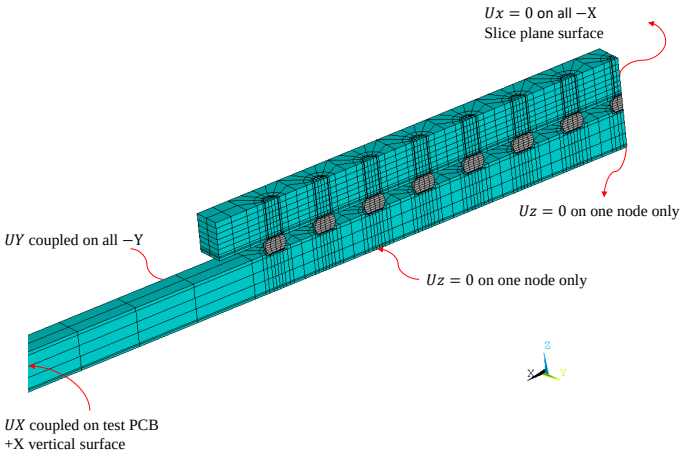

Figure 4: Boundary constraints applied to a typical slice model.

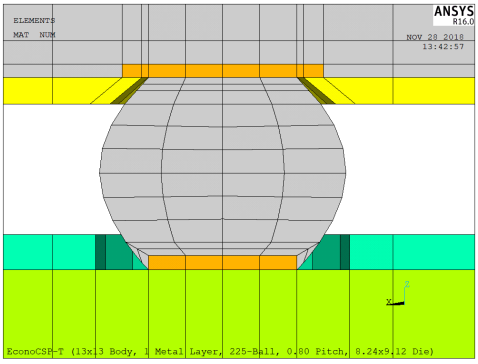

Figure 5: Modeled ball for Chip-Scale package.

4.2. Fatigue Life Prediction Model

Solder balls fatigue life prediction requires combining finite-element simulations with a thermal fatigue methodology. The fatigue methodology is generally obtained by using experimental data and accelerated testing. This methodology is used to determine the number of cycles that a CSP can resist before failure. among the proposed methods, Darveaux [4] was able to establish two equations along with four crack growth correlation constants (K1 through K4), where the finite element simulation results can be used to calculate the crack propagation rate per thermal cycle as well as the number of cycles to crack initiation.

For the methodology application, the singularity issues due to size of the finite element mesh affects the simulation results. However, the analyst must take care to the sensitivity of the finite element simulation. At first, the element thickness at the interface between the balls solder and copper pad must be well controlled. Second, this controlled element thickness technic must be used to determine the element volumetric averaging of the stabilized change in plastic work by which the simulation will be performed. In this respect, Darveaux [4] provided equation constants for varying element thicknesses in the interface. For the present study, the element thickness used was 0.0254 mm (1mil), which is the same value utilized by Zahn [36] in his configurations studies. This thickness is chosen for the first two layers of solder ball material elements at the both interface of solder ball (see figure 5). In the finite element model, Darveaux's methodology requires also that the tape and solder ball material elements not be joined. It is the result of non-adhesion between solder ball and tape materials. Consequently, Darveaux recommends a 0.0127mm (0.5mil) gap between the solder ball and tape material in the finite element model (figure 5). Table 7 present the K1 through K4 crack growth correlation constants for a 0.0254mm (1mil) solder joint element thickness. The equations below (6) and (7) allows to calculate respectively the crack propagation rate per thermal cycle "da/dN" and thermal cycles to crack initiation "No".

$$N_0 = K1(\Delta W_{ave})^{K2} \tag{6}$$

$$\frac{da}{dN} = K3(\Delta W_{ave})^{K4} \tag{7}$$

where "ΔW_{ave}" is the element volumetric average of the stabilised change in plastic work within the controlled eutectic solder element thickness. The characteristic solder joint fatigue life "α" (number of cycles to 63.2% population failure) is expressed as the sum of N_0 and the number of cycles for crack propagation across the entire solder joint diameter "a" as shown in equation 8.

$$\alpha = N_0 + \frac{a}{da/dN} \tag{8}$$

Constant	**Value**
K1	22400cycles/psi
K2	-1.52
K3	5.86×10^{-7}in/cycle/psi
K4	0.98

Table 7: Darveaux K1 through K4 Crack Growth Correlation Constants [4].

4.3. Numerical results and discussion

The ANSYS finite element software led by Anand's viscoplastic constitutive law is used for modeling the slice model of T-CSP displayed in figure 4, the boundary conditions have applied, and the finite element analysis was performed in order to predict the reliability performance of the configuration for T-CSP. The finite element simulation provide the viscoplastic strain energy at printed circuit board solder joints and the package substrate. This viscoplastic strain energy is used to calculate solder balls characteristic life through Darveaux's crack growth rate model.

Once the modeling and the Ansys solution setup was completed, Accelerated thermal cycling (see figure 6), recommended by JEDEC standards [28], are applied as a thermal load in finite element analysis. The temperature profile varies between −40°C and 125°C. Figure 6 shows the thermal cycle loading where the high temperature of the thermal cycle is set as the ANSYS zero strain reference temperature [36]. Two thermal cycles are applied as a loading conditions in the finite element analysis.

Table 8 presents the detailed simulation results of the studied T-CSP configuration. The table shows the position of the failed solder joint in the diagonal section of the submodel (from the centre, including the central solder joint), the variation in viscoplastic deformation energy density when applying the two thermal cycles (i.e. Delta Plastic Work/Cycle), the crack initiation and propagation cycles calculated by equations (6) and (7), and the characteristic life of the solder joint (equation (8)). The results show that the solder joint on the Ball/Substrate Solder Joint broke first with a typical fatigue life of 317 cycles, and that of the solder joints on the PCB is 813 cycles. The failure Ball/Substrate Solder Joint occurred at the Solder Joint number 7, while the failure of the solder joints on the PCB occurred at the solder joints number 8 located at the end of the CSP sub-model (see figure 7).

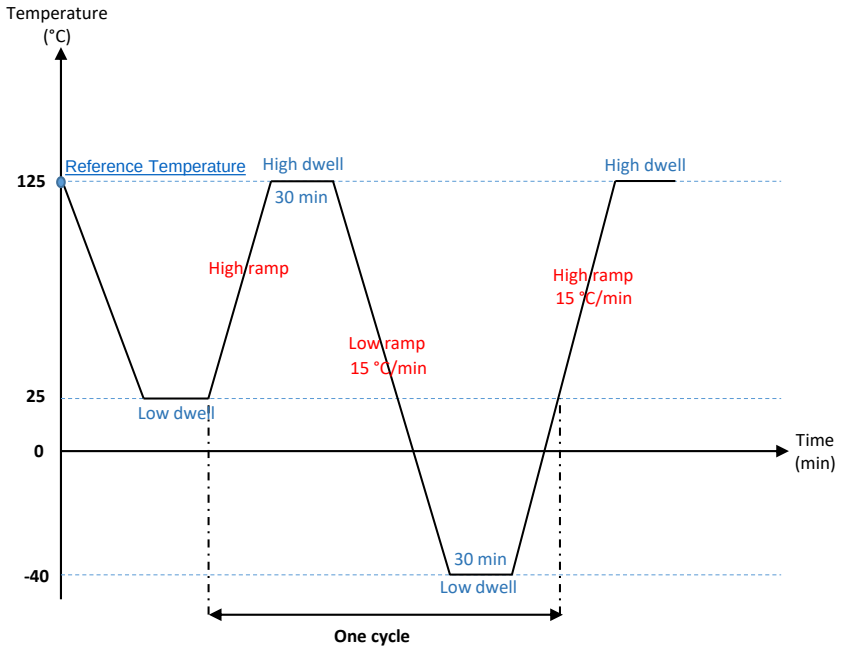

Figure 6: Thermal cycle loading.

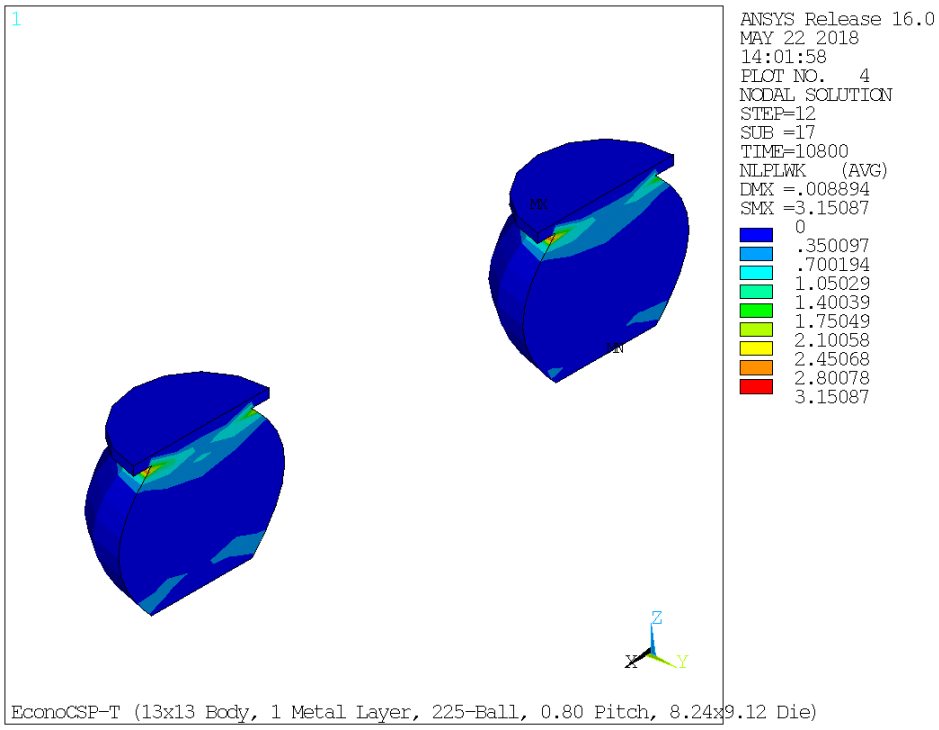

Figure 7: Plastic strain distribution in the solder joints at last loading thermal cycle.

Data Description	**Results**	
	Ball/Substrate Solder Joint	**Ball/Test Board Solder Joint**
Failure Joint (From Center)	7	8
Delta Plastic Work/Cycle (MPa)	0.4987	0.2034
Delta Plastic Work/Cycle (psi)	72.33	29.51
Crack Initiation (cycles)	33	131
Crack Growth Rate (mm/cycle)	0.9883×10^{-03}	0.4104×10^{-03}
Solder Joint Diameter (mm)	0.2800	0.2800
Crack Propagation (cycles)	283	682
Characteristic Life (cycles)	317	813
Model Size Info.		
Total Model Nodes	7035	
Total Model Elements	317	

Table 8: Simulation Results of Chip-Scale Package.

5. Reliability analysis of chip scale packaging

In the T-CSP, the variation of tape vendors and package assembly has an interesting impact on solder joint reliability [36]. However, material parameters composing each configuration show variations due to their uncertain nature [21]. The originality of this paper is to take the material parameters as uncertain variables. These variables are assumed to be subject to the normal probability law. Table 1 shows the random variables of material properties considered in the present study.

Description	Valeur Moyenne	Coefficient de variation	Distribution
Solder ball Elastic Modulus	Table 1.2	0.02	Normal
Solder ball CTE	Table 1.2	0.02	Normal
Solder ball Poisson's Ratio	Table 1.2	0.02	Normal
PCB Core (FR4) Elastic Modulus	Table 1.2	0.02	Normal
PCB Core (FR4) CTE	Table 1.2	0.02	Normal
PCB Core (FR4) Poisson's Ratio	Table 1.2	0.02	Normal
PCB Mask Elastic Modulus	Table 1.2	0.02	Normal
PCB Mask CTE	Table 1.2	0.02	Normal
PCB Mask Poisson's Ratio	Table 1.2	0.02	Normal
Tape (Kapton-E) Elastic Modulus	Table 1.3	0.02	Normal
Tape (Kapton-E) CTE	Table 1.3	0.02	Normal
Tape (Kapton-E) Poisson's Ratio	Table 1.3	0.02	Normal
Conductor (Copper) Elastic Modulus	Table 1.3	0.02	Normal
Conductor (Copper) CTE	Table 1.3	0.02	Normal
Conductor (Copper) Poisson's Ratio	Table 1.3	0.02	Normal

Table 9: The probability parameters of the random variables.

5.1. Design of experiments and Metamodels construction

To construct a metamodel, we need a matrix X which constitutes the design of experiment (DOE) and the corresponding output vector Y. The latter will be computed by passing X through the finite element model. Therefore, it is necessary that the n observations are well distributed over the set of explanatory variables to construct a good metamodel. The purpose of the DOE is to maximize the amount of information obtained from a limited database [10]. In the literature, several methods of DOE are proposed, such as space-flling DOE methods including pseudo-random sampling, orthogonal array sampling, Latin hypercube sampling and quasi-random low-discrepancy sequences [6].

Latin hypercube sampling (LHS) is one of the most widely used methods in DOE [3]. Particularly, an example of a square grid containing possible sampling points is a Latin square if there is only one sample in each row and column. The LHS method is a generalisation of this concept for an arbitrary n dimension.

In practice, to create an LHS sampling of a function of k variables, the range of each variable is divided into n equally probable intervals, then the n sampling points are drawn so that a Latin hypercube is created.

During the exploration stage, it is important to ensure that the created experimental design adequately covers the experimental domain in order to get the most information from the domain using a limited number of points. Therefore, practitioners use certain criteria to study the distance between points to assess the extent to which the distribution is close to a uniform distribution. Among the criteria that can be used to characterize the distribution of points in the experimental domain, two categories can be identified, criteria that are calculated using the distance between pairs of points and discrepancy measures that aim to quantify how the distribution of points differs from a perfectly uniform distribution. **mindist** is a distance measurement that returns the minimum distance between two points of the experimental design. A small **mindist** value means that there is a pair of points that are close, while a large value means that the points are well distributed in the experimental domain. The maximization of **mindist** is called the maximin criterion [8]. This criterion is commonly used to optimize the design of Latin hypercubes to ensure better filling properties of the space. In this work, the **maximinLHS** [8] function is chosen as the method of DOE.

In the created DOE, the number of samples must be correctly defined. Indeed, to determine the correct number of samples, many kriging metamodels are constructed based on different numbers of samples (from 60 to 180) and each metamodel constructed is validated by cross-validation and metamodel

testing methods.

5.2. Metamodels validation

Before the operation stage, the constructed metamodel needs to be validated. The type of constructed metamodel, its quality, and the quantity of data are tree issues that affect the accuracy of metamodel. There are several methods to assess the accuracy of the built metamodel, which known as metamodel validation. The most used methods for assessing metamodel accuracy and comparing it with others, are model testing and Cross Validation (CV).

5.2.1. Metamodel testing

To evaluate the performance of metamodel, the simple way is to examine its residual errors[11]. Model testing methods is applied at a set of observations that are not used in the metamodel construction, it aims to measure the difference between the observed values y and the values predicted by the built metamodel $\hat{y}$. The residual error is smaller, the smaller the fitting error is. The root mean squared error (RMSE), which is a global error measure, is the most popular method:

$$\mathrm{RMSE} = \sqrt{\frac{1}{n}\sum_{i=1}^{n}\left(y^{(i)} - y^{(i)}\right)^2} \tag{9}$$

Moreover, the coefficient of determination R^2 is another commonly used error method; it provides a measure of how well observed outcomes are replicated by the model. Otherwise, lets $y^{(i)}$, the experimental response, $\hat{y}^(i)$ the predicted response and $\bar{y}$ represent the mean of the response. The coefficient R^2 is expressed as:

$$R^2 = 1 - \frac{\sum_{i=1}^{n}\left(y^{(i)} - \hat{y}^{(i)}\right)^2}{\sum_{i=1}^{n}\left(y^{(i)} - \bar{y}^{(i)}\right)^2} = \frac{\sum_{i=1}^{n}\left(\hat{y}^{(i)} - \bar{y}^{(i)}\right)^2}{\sum_{i=1}^{n}\left(y^{(i)} - \bar{y}^{(i)}\right)^2} \tag{10}$$

Where $0 \leq R^2 \leq 1$. The built metamodel is more accurate when R^2 is closer to 1.

5.2.2. Cross-validation

Cross-validation (CV) is a method to evaluate the quality of a metamodel and/or to compare it with others. The concept is to use the same sample for the construction and validation of the metamodel. Cross-validation consists in randomly dividing the set of samples generated by the DOE into equal subsets, to exclude one of these subsets each iteration and construct the metamodel based on the remaining subsets. The resulting errors of each iteration between the constructed metamodel, and the excluded sub-set are computed and summed [9]. This sum is defined as the cross-validation error, called p-fold error, for the metamodel. The "leave-k-out" approach is a cross-validation variant in which all possible subsets of size k are discarded, and the metamodel is constructed on the basis of the remaining set, and in each case the error is evaluated at the discarded subsets. Particularly, in the case where $k = 1$, the cross-validation is called "Leave-one-out" [15], and the cross-validation prediction of the root mean squared error (RMSE) error and the maximum absolute error ($\mathrm{MAE_{CV}}$) are separately defined by:

$$\mathrm{RMSE_{CV}} = \sqrt{\frac{1}{n}\sum_{i=1}^{n}\left(y^{(i)} - y_{-i}^{(i)}\right)^2} \tag{11}$$

$$\mathrm{MAE_{CV}} = \frac{1}{n}\sum_{i=1}^{n}\left|y^{(i)} - y_{-i}^{(i)}\right| \tag{12}$$

Where $y^{(i)}$ is the exact response of the FE model at $x^{(i)}$ and $y^{(i)}_{-i}$ is the prediction at $x^{(i)}$ of the constructed metamodel based on all the points of the sample except $\left(x^{(i)}, y^{(i)}\right)$.

5.2.3. Validation results

The results of metamodels validation are plotted in Figure 8. It can be seen that the initial sample size could be set as 180 since the Kriging metamodel performance would not significantly improve when the sample size is larger than 160. The metamodel validation for a Kriging metamodels built based on 180 samples are $RMSE_{CV} = 3.3$, $MAE_{CV} = 2.42$ and $R^2 = 0.9$ for Ball/Substrate Solder Joint, and $RMSE_{CV} = 1.79$, $MAE_{CV} = 1.30$ and $R^2 = 0.89$ for Ball/Test Board Solder Joint. This also indicates that the built metamodel according to 180 samples is sufficiently accurate.

5.3. Monte Carlo Simulation based Metamodel

The last step of the probabilistic method, after metamodel construction and validation, is the Monte Carlo simulation (MCS). The MCS application consists of generating a sampling of random variables with the R software and computing the response with the built kriging metamodel.

The MCS results for the Ball/Substrate Solder Joint and the Ball/PCB Solder Joint are shown in Figures 9 and 10 respectively. The results are composed of four graphs of the adjustment quality provided by the functions denscomp, qqcomp, cdfcomp and ppcomp of the "fitdistrplus" package of the R :

- a density plot representing the density function of the fitted distribution along with the histogram of the empirical distribution,
- a **CDF** plot of both the empirical distribution and the fitted distribution,
- a **Q-Q** plot representing the empirical quantiles (y-axis) against the theoretical quantiles (x-axis)
- a **P-P** plot representing the empirical distribution function evaluated at each data point (y-axis) against the fitted distribution function (x-axis).

The results show that MCS based on the kriging metamodel is more practical and efficient than a conventional MCS simulation method based on the finite element model. The computation time required for a deterministic simulation with the T-CSP finite element model is about 4 minutes (240s). To perform an MCS with 10^6 samples from the finite element model, the calculation time is about 4×10^6 minutes. If the MCS is based on the kriging metamodel, the computation time is significantly reduced, which makes the probabilistic method affordable.

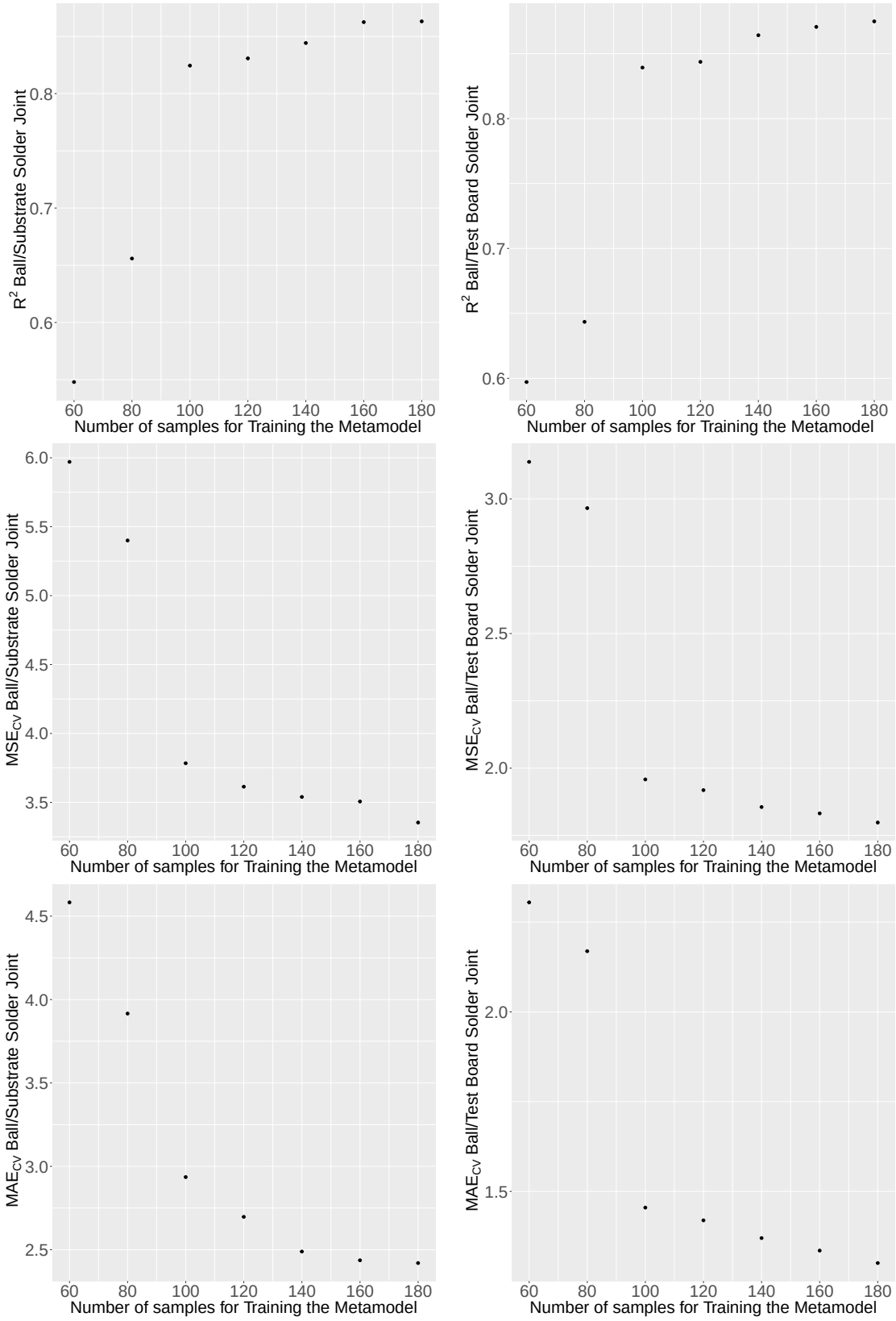

Figure 8: Kriging metamodels validation for reliability prediction of T-CSP.

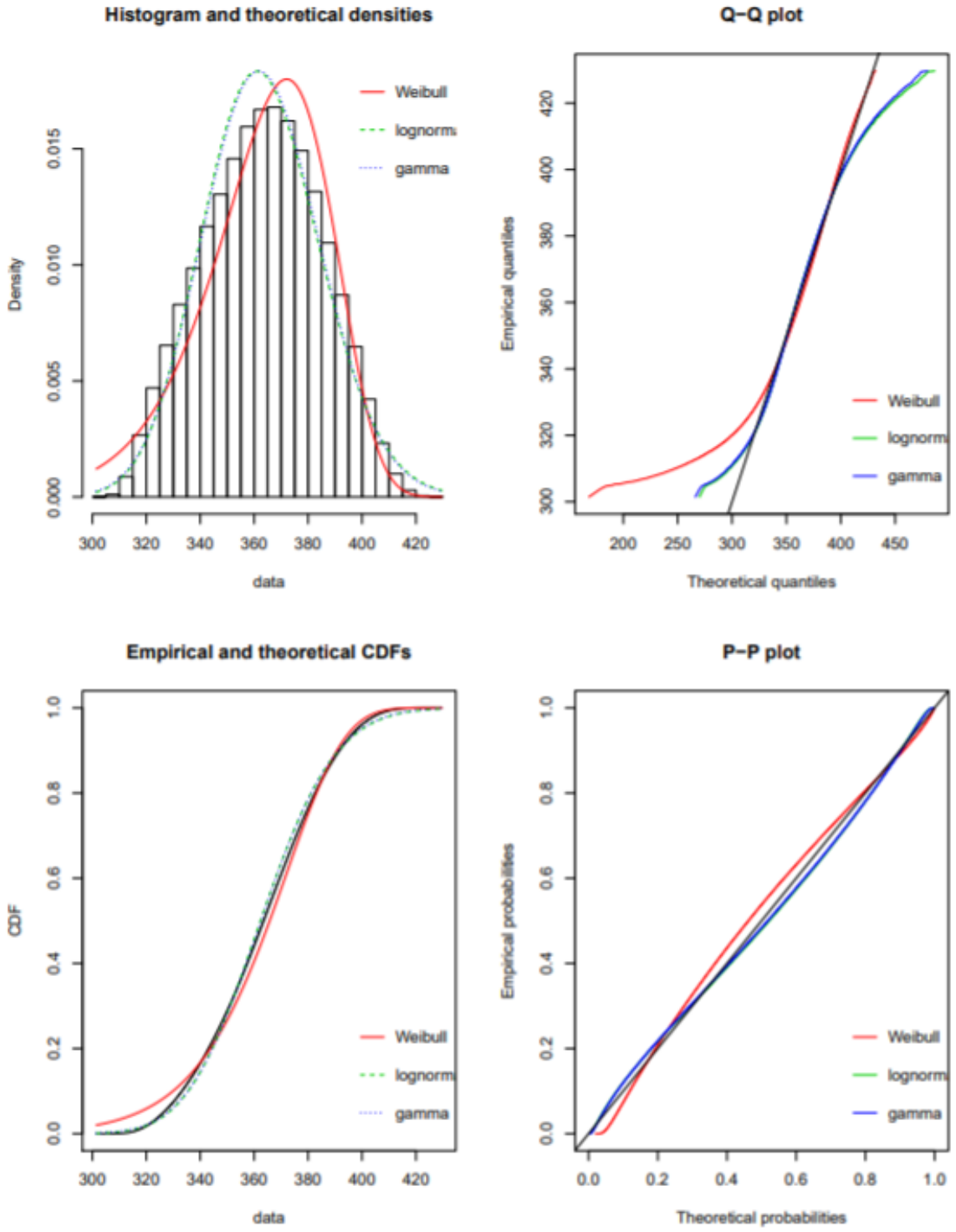

Figure 9: Four Goodness-of-fit plots for various distributions fitted to continuous data (Weibull, gamma and lognormal distributions) in Ball/Test Board Solder Joint

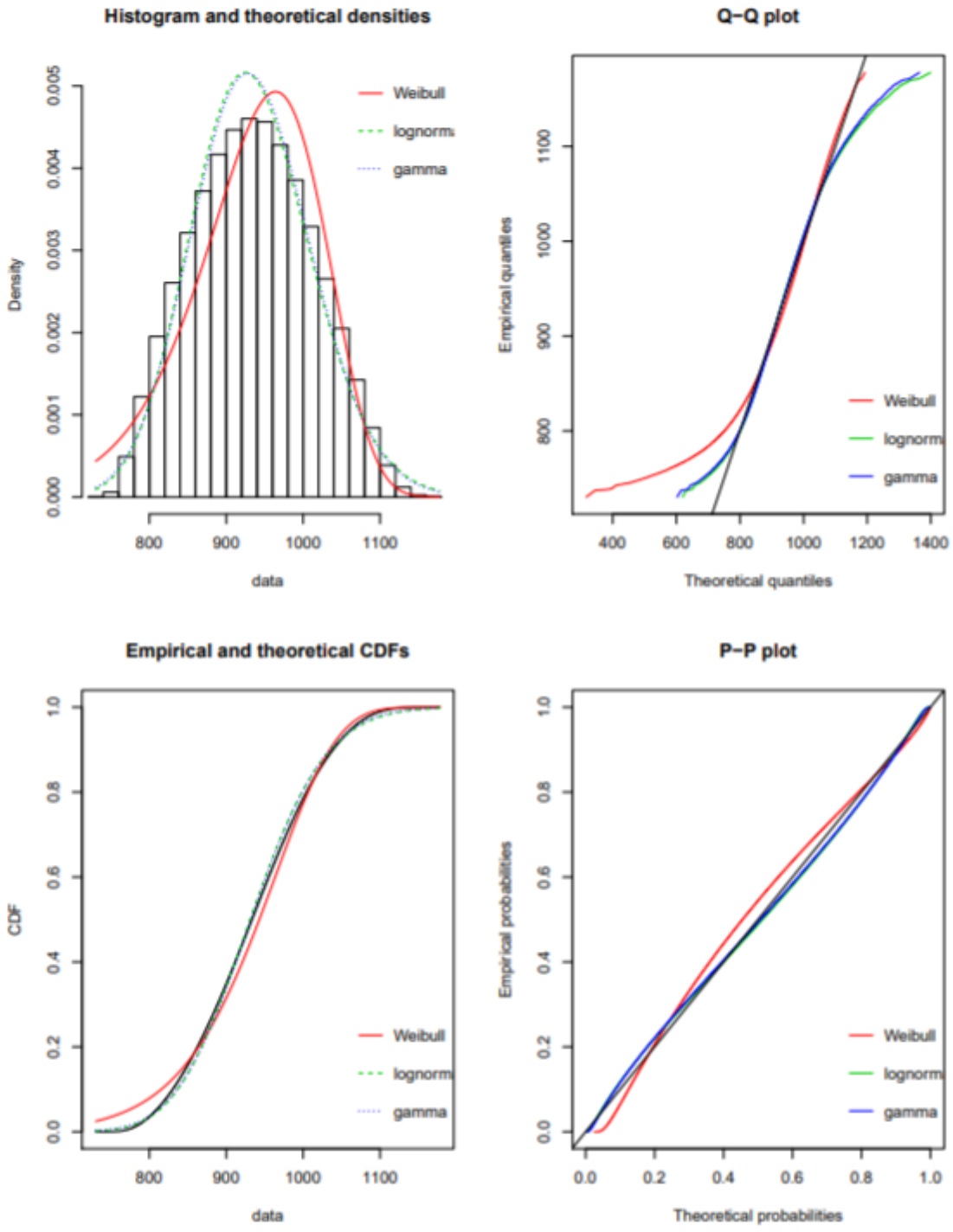

Figure 10: Four Goodness-of-fit plots for various distributions fitted to continuous data (Weibull, gamma and lognormal distributions) in Ball/Substrate Solder Joint

6. Conclusion

This paper focused on the application of metamodel based probabilistic method in the reliability assessment of T-CSP. The finite element analysis is performed to predict the reliability performance of CSP through accelerated temperature cycling solder joint characteristic fatigue life. Darveaux's crack growth rate model was applied to calculate solder joint characteristic life using simulated viscoplastic strain energy density results at the package substrate and printed circuit board solder joints. To avoid tedious calculation, kriging metamodel is used carefully to approximate the relationship between the response and input variables. Then, metamodel based probabilistic method, which combine the MCS and the constructed metamodel, was presented and applied to take into account the uncertainties in the reliability analysis of T-CSP.

References

[1] Anand, L. Constitutive equations for the rate-dependent deformation of metals at elevated temperatures. *Journal of Engineering Materials and Technology(Transactions of the ASME) 104*, 1 (1982), 12–17.

[2] ANSYS Guide, . *ANSYS Structural Analysis Guide*, 2016.

[3] Ben Abdessalem, A., and El-Hami, A. Global sensitivity analysis and multi-objective optimisation of loading path in tube hydroforming process based on metamodelling techniques. *The International Journal of Advanced Manufacturing Technology 71*, 5 (Mar 2014), 753–773.

[4] Darveaux, R. Effect of simulation methodology on solder joint crack growth correlation. In *Electronic Components & Technology Conference, 2000. 2000 Proceedings. 50th* (2000), IEEE, pp. 1048–1058.

[5] Darveaux, R., Banerji, K., Mawer, A., and Dody, G. Reliability of plastic ball grid array assembly, 1995.

[6] Dean, A., Morris, M., Stufken, J., and Bingham, D. *Handbook of design and analysis of experiments*, vol. 7. CRC Press, 2015.

[7] Dubourg, V., Deheeger, F., and Sudret, B. Metamodel-based importance sampling for the simulation of rare events. *Applications of Statistics and Probability in Civil Engineering 26* (2011), 192.

[8] Dupuy, D., Helbert, C., Franco, J., et al. Dicedesign and diceeval: Two r packages for design and analysis of computer experiments. *Journal of Statistical Software 65*, 11 (2015), 1–38.

[9] Forrester, A., Keane, A., et al. *Engineering design via surrogate modelling: a practical guide*. John Wiley & Sons, 2008.

[10] Giunta, A. A., Wojtkiewicz, S. F., Eldred, M. S., et al. Overview of modern design of experiments methods for computational simulations. In *Proceedings of the 41st AIAA aerospace sciences meeting and exhibit, AIAA-2003-0649* (2003).

[11] Hamdani, H., Radi, B., and El Hami, A. Métamodélisation pour une conception robuste des systèmes mécatroniques. *Incertitudes et fiabilité des systèmes multiphysiques 2*, Numéro 2 (2017), 10.

[12] Hamdani, H., Radi, B., and El Hami, A. Metamodel assisted evolution strategies for global optimization of solder joints reliability in embedded mechatronic devices. *Microsystem Technologies* (Jun 2019).

[13] Hamdani, H., Radi, B., and El Hami, A. Optimization of solder joints in embedded mechatronic systems via kriging-assisted cma-es algorithm. *International Journal for Simulation and Multidisciplinary Design Optimization 10* (2019), A3.

[14] Hayes, K. *Uncertainty and uncertainty analysis methods*. CSIRO, 2011.

[15] Huang, C., Radi, B., and El Hami, A. Uncertainty analysis of deep drawing using surrogate model based probabilistic method. *The International Journal of Advanced Manufacturing Technology 86*, 9-12 (2016), 3229–3240.

[16] Huang, C., Radi, B., El Hami, A., and Bai, H. Cma evolution strategy assisted by kriging model and approximate ranking. *Applied Intelligence 48*, 11 (Nov 2018), 4288–4304.

[17] Jannoun, M., Aoues, Y., Pagnacco, E., Pougnet, P., and El-Hami, A. Probabilistic fatigue damage estimation of embedded electronic solder joints under random vibration. *Microelectronics Reliability 78* (2017), 249–257.

[18] Jin, R., Du, X., and Chen, W. The use of metamodeling techniques for optimization under uncertainty. *Structural and Multidisciplinary Optimization 25*, 2 (Jul 2003), 99–116.

[19] Lee, W., Nguyen, L., and Selvaduray, G. S. Solder joint fatigue models: review and applicability to chip scale packages. *Microelectronics reliability 40*, 2 (2000), 231–244.

[20] Lin, J. Modeling test responses by multivariable polynomials of higher degrees. *SIAM Journal on Scientific Computing 28*, 3 (2006), 832–867.

[21] Makhloufi, A., Aoues, Y., and El Hami, A. Reliability based design optimization of wire bonding in power microelectronic devices. *Microsystem Technologies 22*, 12 (2016), 2737–2748.

[22] Makhloufi, A., Aoues, Y., ElHami, A., Radi, B., Pougnet, P., and Delaux, D. 10 - study on the thermomechanical fatigue of electronic power modules for traction applications in electric and hybrid vehicles (igbt). In *Reliability of High-Power Mechatronic Systems 1*, A. E. Hami, D. Delaux, and H. Grzeskowiak, Eds. Elsevier, 2017, pp. 213 – 251.

[23] Matheron, G. Principles of geostatistics. *Economic geology 58*, 8 (1963), 1246–1266.

[24] Nubli Zulkifli, M., Azhar Zahid Jamal, Z., and Abdul Quadir, G. Temperature cycling analysis for ball grid array package using finite element analysis. *Microelectronics International 28*, 1 (2011), 17–28.

[25] Pao, Y.-H. A fracture mechanics approach to thermal fatigue life prediction of solder joints. *IEEE Transactions on Components, Hybrids, and Manufacturing Technology 15*, 4 (1992), 559–570.

[26] Rasmussen, C. E., and Williams, C. K. *Gaussian processes for machine learning*, vol. 1. MIT press Cambridge, 2006.

[27] Sacks, J., Welch, W. J., Mitchell, T. J., and Wynn, H. P. Design and analysis of computer experiments. *Statistical science* (1989), 409–423.

[28] Standard, J. Jesd22-a104-b. *Temperature Cycling, July* (2000).

[29] Subrahmanyan, R. *A damage integral approach for low-cycle isothermal and thermal fatigue*. Cornell University, May, 1990.

[30] Sudret, B. Meta-models for structural reliability and uncertainty quantification. *arXiv preprint arXiv:1203.2062* (2012).

[31] Syed, A. R. Creep crack growth prediction of solder joints during temperature cycling—an engineering approach. *Journal of Electronic Packaging 117*, 2 (1995), 116–122.

[32] Team, R. C. R: A language and environment for statistical computing. r foundation for statistical computing, vienna, austria. 2013, 2014.

[33] Wu, J., Luo, Z., Zhang, Y., and Zhang, N. An interval uncertain optimization method for vehicle suspensions using chebyshev metamodels. *Applied Mathematical Modelling 38*, 15-16 (2014), 3706–3723.

[34] Wu, J., Luo, Z., Zheng, J., and Jiang, C. Incremental modeling of a new high-order polynomial surrogate model. *Applied Mathematical Modelling 40*, 7 (2016), 4681 – 4699.

[35] Zahn, B. A. Comprehensive solder fatigue and thermal characterization of a silicon based multi-chip module package utilizing finite element analysis methodologies. In *Proceedings of the 9th International ANSYS Conference and Exhibition* (2000), pp. 1–15.

[36] Zahn, B. A. Impact of ball via configurations on solder joint reliability in tape-based, chip-scale packages. In *Electronic Components and Technology Conference, 2002. Proceedings. 52nd* (2002), IEEE, pp. 1475–1483.